Effect of Li Doping on Structural, Optical, and Electrical Properties of CuO Thin Films Produced by Spray Pyrolysis Method

N. Allouche[a,*], B. Boudjema[a,b], R. Daira[a,b] and F. Bayansal[c]

[a]*Department of Physics, Faculty of Sciences, University of 20 August 1955, BP 26 El hadaiek, 21000, Skikda, Algeria*
[b]*Physical Chemistry Research on Surfaces and Interfaces Lab., University of 20 August 1955, BP 26 El hadaiek, 21000, Skikda, Algeria*
[c]*Electrical & Computer Engineering Department, University of Connecticut, 371 Fairfield Way, Storrs, Connecticut, 06269-4157, United States*

In the present work, structural, optical, and electrical properties of lithium-doped (0–6 at.%) copper oxide thin films were investigated. The films were obtained by the spray pyrolysis method on glass substrates at 450°C. The X-ray diffraction method, UV-visible spectroscopy, and the four-point probe technique were used to analyze the films. Based on the X-ray diffraction investigations, it was found that the polycrystalline films have monoclinic phases with preferred (111) and ($\bar{1}$11) crystallographic planes. The incorporation of lithium doping into the copper oxide thin film yielded crystallite sizes of approximately 2 nm. The estimated optical band gap values are decreased from 1.88 to 1.64 eV with increasing lithium concentration. Four-point probe studies revealed that the resistivity of the films decreased from 339 to 186 K Ω cm with increasing lithium concentration.

topics: CuO, Li doping, spray pyrolysis, thin film

1. Introduction

Researchers have become interested in investigating transition metal oxides due to their significant impact on technological and applied sciences, particularly copper oxides. Copper oxide (CuO) is a p-type semiconductor with a monoclinic structure and a band gap of 1.2–1.7 [1, 2]. It has interesting structural, electrical, and optical properties that encourage its use in a number of applications, including solar cells [3], sensors [4], catalysts [5], microwave insulation materials [6], high-temperature superconductors [7], and lithium-ion batteries [8]. The battery industry relies on lithium for its high energy density and storage capacity. This is why scientists have been interested in mixing lithium with numerous metal oxides such as CuO [9] and SnO_2 [10], as these materials play an effective role in battery applications and energy storage. Studies have shown that lithium has a significant effect on the electrical and optical properties of metal oxides [11, 12]. Researchers are interested in studying the doping of CuO with monovalent atoms such as Li, K, and Na [13, 14] due to its ability to act as a p-type activator, leading to an increase in Cu^{+2} ion density. In addition to increasing the electrical conductivity of CuO thin films, Li^+ can be significantly grafted onto

CuO due to the high similarity of their ionic radii of Li^+ (0.76 Å) [15, 16] and Cu^{+2} (0.73 Å) [15, 17]. Various methods have been used to obtain CuO thin films, including spray pyrolysis [2, 18–20], chemical vapor deposition [19], sol–gel solution [20], pulsed laser deposition [21], thermal oxidation [22], electrochemical deposition [23], and molecular beam epitaxy [24].

It is known that the optical, electrical, and structural properties of metal oxides are affected by different doping. In their studies, Xu et al. [25] found that Mn doping caused modifications to the structural and magnetic properties of CuO. In another study, Bayansal et al. [26] stated that when Co doping increased, the crystallite size of the CuO films decreased. On the other hand, Basith et al. [27] stated that Ni doping resulted in an enhancement in the band gap of CuO. Bayansal et al. [28] reported similar conclusions in their study on Pb-doped CuO thin films. Kadhim et al. [29], in the study on Li-doped CuO thin films prepared by sol–gel method using the spin coating technique, show that the CuO and CuO-doped Li present a monoclinic structure and the value of the band gap decreases with the increase in the concentration of Li. Wang et al. [30] studied the enhancement of CuO nanostructured properties. They found that
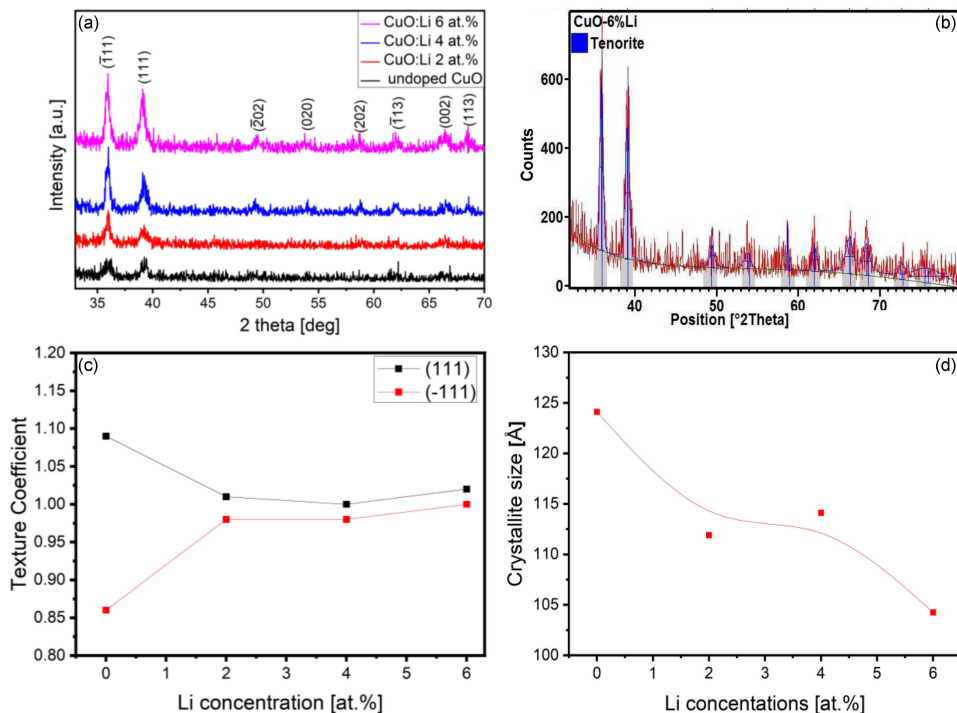
Fig. 1. (a) XRD patterns of pure and Li-doped (2, 4, and 6 at.%) CuO thin films. (b) Adjustment of CuO 6% Li thin film diffractograms performed using the HighScore software. (c) Texture coefficient variation as a function of Li concentration for (111) and ($\bar{1}$11) planes. (d) Variation of the average crystallite size with Li doping.

Li doping increased energy density while maintaining high power density and long-term cyclability. In the study by F. Bayansal et al. [31], thin films of Li-doped CuO were prepared using the successive ionic layer adsorption and reaction (SILAR) method in order to improve their properties. It was reported that as the concentration of Li increased, films with a uniform surface and smaller particle size were obtained. On the other hand, Li-doped CuO thin films were prepared by spray pyrolysis for the application of electrodes in photoelectrochemical cells by Chia-Ying Chiang et al. [32].

Our present work focuses on producing pure and Li-doped CuO thin films using the spray pyrolysis method. This method offers a number of advantages, including low cost, rapid processing, and the ability to obtain high-quality thin films on large surfaces. The aim was to observe the effect of Li on the stability of the CuO phase. The structural, optical, and electrical properties of the films have been investigated using X-ray diffraction, UV-visible spectroscopy, and four-point probe method.

2. Experimental details

The spray pyrolysis method was used to deposit CuO thin films on glass substrates. The copper(II) acetate dihydrate ($CU(CO_2CH_3)_2 \cdot 2H_2O$, Sigma-Aldrich) was used as a precursor at a concentration of 0.1 M. Prior to deposition, glass substrates were washed with deionized (DI) water, methanol, and acetone in an ultrasonic bath for 15 min at room temperature to remove traces of organic residues. Lithium chloride (LiCl, Sigma-Aldrich) was used as the salt source of Li doping atoms. The atomic ratio of the Li was adjusted to be 2, 4, and 6% by adding LiCl to the starting solution. The nozzle–substrate distance was set to 25 cm, the substrate temperature was set to 450°C, and the thickness of these films is estimated to be 400 nm. The prepared samples were then subjected to a series of characterizations to investigate the effect of Li doping on the properties of CuO films using a Bruker D8 ADVANCE X-ray diffractometer, a Keithley 2400 SourceMeter, and a Shimadzu UV-1700 spectrophotometer, respectively.

3. Results and discussions

3.1. Structural characterization

The X-ray diffraction (XRD) patterns of the films are shown in Fig. 1a. The analysis revealed that the films have polycrystalline structures with stable monoclinic phases that are members of the $C2/c$ space group (JCPDS file No. 001-1117). All sample patterns exhibited 2 intense peaks located at 35.88° and 39.06° assigned to the planes ($\bar{1}$11) and (111), respectively. The intensity of the diffraction

TABLE I

Structural parameters of Li-doped CuO thin films.

Li concentrations [at.%]	2θ [°]	FWHM	d_{hkl} [Å]	D [Å]	D_{mean} [Å]	ε [%]	δ ($\times 10^{-3}$) [1/nm^2]	(hkl)
0	35.96	0.676	2.497	115.272	124.109	0.31	7.5257	(-111)
	39.39	0.909	2.293	132.945		0.40	5.6578	(111)
2	35.97	0.307	2.498	118.526	111.899	0.41	7.1181	(-111)
	39.05	0.512	2.304	134.905		0.63	5.4947	(111)
4	35.98	0.451	2.498	105.272	114.109	0.66	9.0234	(-111)
	39.09	0.758	2.304	122.945		0.83	6.6157	(111)
6	35.88	0.471	2.500	117.362	104.249	0.65	7.2601	(-111)
	39.06	0.612	2.304	91.1356		0.83	12.04	(111)

peaks increased with Li doping, confirming that the crystallinity was improved. There are other studies reporting that increasing the doping ratio has a generative effect on crystallinity [33, 34]. A similar improvement was also observed in the small peaks of planes ($\bar{2}02$), (020), (202), ($\bar{1}13$), (022), and (113). No impurity peaks were detected, meaning that lithium ions were incorporated into the copper sites of the lattice, see Fig. 1b. Observation of monoclinic structure in all samples confirmed that doping affected the diffraction intensity of the peaks but not the crystal structure of CuO.

The texture coefficients are calculated from the XRD data by using the equation [35]

$$TC_{(hkl)} = \frac{\left(I_{(hkl)}/I_{o(hkl)}\right)}{\frac{1}{N}\sum_N \left(I_{(hkl)}/I_{o(hkl)}\right)}, \tag{1}$$

where $I_{o(hkl)}$ is the standard relative intensity, $I_{(hkl)}$ is the measured intensity, and N is the number of reflections. The texture coefficients of ($\bar{1}11$) and (111) planes were calculated, and their changes with increasing Li doping are plotted in Fig. 1c. It was observed that the texture coefficient of the (111) plane was greater than unity, which decreased with increasing doping rate up to 2 at.% of Li and stabilized around unity. It is known that an enhancement in the texture coefficient denotes an increased number of grains along the plane. Therefore, it can be concluded that Li doping reduces the number of grains at low concentrations but increases it again at high concentrations. However, a similar behavior was observed in the ($\bar{1}11$) plane. It is also clear from Fig.1(c) that (111) and ($\bar{1}11$) planes are the preferential orientation for Li-doped CuO films compared to the pure CuO. Naveena et al. [36] and Prabu et al. [37] also reported in their studies that the (111) plane is the preferential orientation of the CuO films.

The crystallite sizes (D) of the films were obtained from the two intense peaks using the Debye–Scherer equation [38]

$$D = \frac{0.89\lambda}{\beta\cos(\theta)}, \tag{2}$$

where $\lambda = 1.54056$ Å is the wavelength, θ is the Bragg's angle of the peaks, β is the full width at half maximum (FWHM). The crystallite size of

the samples is influenced by the Li concentration, as shown in Fig. 1d. The average crystallite size (D_{mean}) values are found to be 124, 112, 114, and 104 Å for 0, 2, 4, and 6 at.% Li-doped films, respectively. As can be seen from the structural parameters listed in Table I and Fig. 1d, the Li doping caused larger crystallites to form. The dislocation density (δ) and the strain (ε) were obtained using the equations [39]

$$\delta = \frac{1}{D^2}, \tag{3}$$

$$\varepsilon = \frac{\beta\cos(\theta)}{4}. \tag{4}$$

Strain (ε) and dislocation density (δ) values belonging to ($\bar{1}11$) and (111) planes are given in Table I. As can be seen, the Li doping caused a slight decrease in both parameters. Moreover, an inversely proportional relationship between strain and size of the crystallites was observed. The strain (ε) and dislocation density (δ) values are enhanced due to the increase in the number of grains and decrease in crystallite size with Li doping. This change can also be explained by the difference in the ionic radii between lithium Li$^+$ (0.76 Å) and copper Cu^{2+} (0.73 Å) ions. Similar results, comparable to those obtained here, were also found by Shannon et al. [40]. However, attenuated strain suggests a reduction in the lattice defects concentration. Accordingly, due to the fact that these two quantities are related to the dislocation networks, their decrease is synonymous with better crystalline quality. This means that the doped films have smaller microstain values, which may denote a slight enhancement in crystallinity. Similar conclusions supporting this effect were also reported by Bayansal et al. [31].

The lattice parameters a, b, c for a monoclinic structure are evaluated using the following equation

$$\frac{1}{d_{hkl}^2} = \frac{1}{\sin^2(\beta S)}\left(\frac{h^2}{a^2} + \frac{l^2}{c^2} - \frac{2hl}{ac}\right) + \frac{k^2}{b^2}, \tag{5}$$

where the values a, b, c denote the lattice parameters, (hkl) are the Miller indices, d is the interplanar distance, and β is 99.48° for the monoclinic structure. The calculated lattice constants for the films are given in Table II, where the standard

TABLE II

Lattice constants for pure CuO and Li-doped CuO films.

Li [at.%]	a [Å]	b [Å]	c [Å]	a/b	c/b
0	4.643	3.412	5.112	1.361	1.498
2	4.643	3.406	5.101	1.363	1.498
4	4.671	3.402	5.118	1.373	1.504
6	4.641	3.409	5.095	1.361	1.494
JCPDS No. 001-1117	4.653	3.410	5.108	1.364	1.498

values of the constants, $a = 4.6530$ Å, $b = 3.410$ Å, and $c = 5.1080$ Å were used (JCPDS file No. 001-1117). It is obvious that the constants calculated in this study are very close to the standard values. This might be due to the variation of the lattice constants resulting from the fact that CuO has a complex monoclinic structure and the strains that occurred during the formation of the films. However, the increase in Li concentration led to a slight increase in the lattice constants. At 4 at.% of Li doping, the lattice constant, a, reached 4.671 Å. The observed increase in the parameter a can be attributed to the different ionic radii of Cu^{2+} and Li^+.

3.2. Optical characterization

Highlights of the optical transmittance with respect to the wavelength in the spectral range from 300 to 900 nm are presented in Fig. 2a. The spectrum of pure film exhibited a maximum (about 70%) around 780 nm. On the other hand, it decreased with increasing Li doping and reached a minimum (about 50%) when Li concentration was 6 at.%. This range of transparency corresponds to an acceptable absorption in CuO due to the transitions between the valence and the conduction band. The decrease in the transmittance originates from the increase in the surface roughness of the films. Similar results are outlined by Naveena et al. [36] and Hussin et al. [41]. The band gap (E_g) of the material can be calculated from the Tauc equation [42]

$$(\alpha h\nu)^n = A(h\nu - E_g), \qquad (6)$$

where n is related to the transition type (equal to 2 and 1/2 for direct and indirect transitions, respectively). To obtain the E_g values, the Tauc plot that shows the variation of $(\alpha h\nu)^2$ with respect to the photon energy ($h\nu$) was drawn. The E_g values were obtained by extrapolating the linear part and finding the interception point of the plots with the x-axis in Fig 2b.

The estimated E_g values of the films were found to be 1.88, 1.79, 1.72, and 1.64 eV, and they are shown in Fig. 3. At increasing Li concentrations, E_g is reduced from 1.88 to 1.64 eV. This is in good accordance with previously reported data [43, 44]. This decrease can be attributed to variations in the crystallite size and Li ions adopting substitution position sites in the CuO lattice. When Li is doped
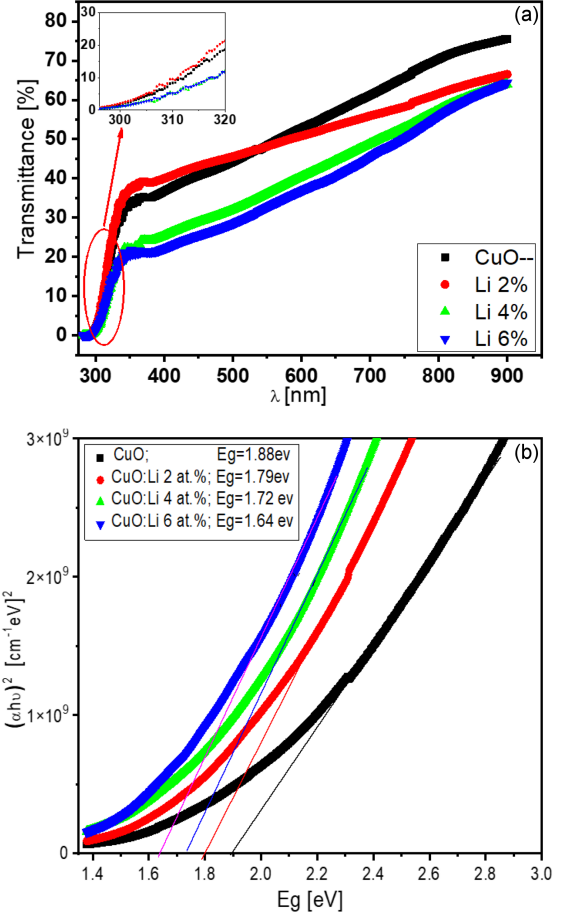

Fig. 2. (a) Transmittance spectrum for pure and Li-doped CuO. (b) Band gap variation of pure CuO and Li-doped CuO films.

into CuO, the optical energy band gap decreases due to band tail effects. This is because the donor density increases in parallel with the increase in the ratio of Li added to the structure. This can result in the creation of tail-like states extending below the conduction band [45].

3.3. Electrical characterization

The electrical properties of thin films are of considerable interest in several applications, such as gas sensors and solar cells. Among them, resistivity is one of the most important parameters to be studied in transparent and conductive oxides. Therefore, the resistivity of the films was measured at room temperature in the dark using the four-point probe method. Figure 4 shows the variation of the resistivity of the films with respect to Li concentration. The results reveal that the resistivity of the films decreased from 339 to 186 K Ω with increasing Li concentration. The decrease in resistivity may also be due to these reasons: (i) improved crystallization, (ii) interstitial position of Li ions, and (iii) reduction in the carrier scattering as a consequence of the
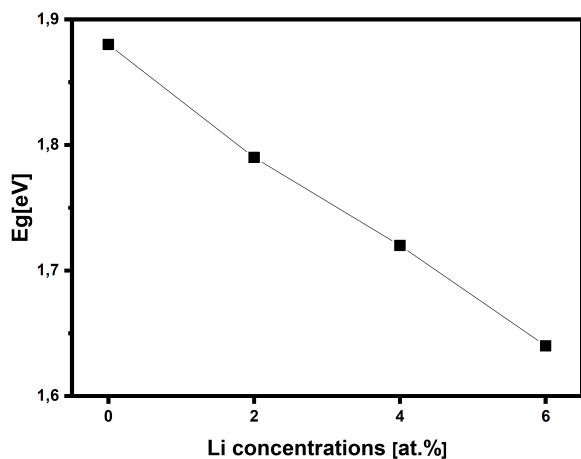
Fig. 3. Behavior of direct band gap energy of the films with respect to the Li concentration.
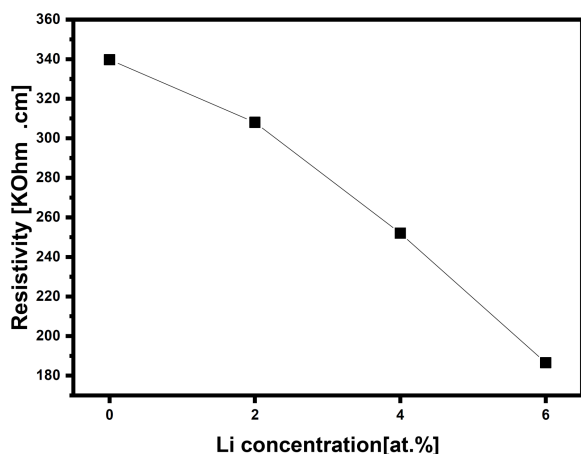

Fig. 4. The variation in resistivity of CuO films with respect to Li concentration.

decrease in the number of grains. Anand et al. [46] and Khodair et al. [47] reported comparable results to the resistivity values calculated in this study.

4. Conclusions

In the current research paper, the influence of Li doping on the structural, optical, and electrical properties of CuO thin films deposited onto glass substrates through the use of the spray pyrolysis method was investigated. The XRD analysis revealed that the synthesized CuO thin films have pure polycrystalline structures with monoclinic phases. Two preferential orientations along (111) and ($\bar{1}$11) are indicated. From the optical investigations, it was found that the transmittance of the films decreased with increasing Li concentrations. Furthermore, Li doping caused a decrease in the direct optical gap values from 1.88 to 1.64 eV. The four-point probe measurement revealed a decrease in the resistivity values of the films with

increasing Li concentration. This study aimed to support the developments in electronic devices and photonic technologies and their use in potential applications by investigating the effect of lithium concentration on the structural, optical, and electrical properties of copper oxide thin films.

References

[1] A. Chen, H. Long, X. Li, Y. Li, G. Yang, P. Lu , *Vacuum* **83**, 927 (2009).

[2] N. Allouche, B. Boudjema, R. Daira, M. Abdelkader, *J. Ovonic. Res.* **19**, 369 (2023).

[3] T.F. Yadeta, T. Imae, *Appl. Surf. Sci.* **637**, 157880 (2023).

[4] F. Bayansal, M.T. Yuksel, S. MacDougall, A. Ahmadi, *Ceram. Int.* **50**, 5140 (2023).

[5] S. Shao, W. Wang, X. Yang, Z. Ye, J. Sun, X. Li, *Fuel* **353**, 129028 (2023).

[6] D.W. Kim, B. Park, J.H. Chung, K.S. Hong, *Jpn. J. Appl. Phys.* **39**, 2696 (2000).

[7] C.M. Cheong, S.K. Chen, *Mater. Today Proc.* **96**, 94 (2024).

[8] Q. Wang, Z. Chen, S. Bai, X. Wang, Y. Zhang, *J. Alloys Compd.* **958**, 170485 (2023).

[9] A. Torrisi, G.Ceccio, J.Vacik, V. Lavrentiev, *Chemosensors* **9**, 246 (2021).

[10] G. Goward, L. Nazar, W. Power, *J. Mater. Chem.* **10**, 1241 (2000).

[11] I.A. Garduño, J.C. Alonso, M. Bizarro, R. Ortega, L.R. Fernández, A. Ortiz, *J. Cryst. Growth* **312**, 3276 (2010).

[12] Y. Zhao, H. Wang, X. Gong, J. Wang, H. Li, M. Tang, X. Li, *Vacuum.* **137**, 56 (2017).

[13] Prakash Chand, Anurag Gaur, Ashavani Kumara, Umesh Kumar Gaur, *Appl. Surf. Sci.* **307**, 280 (2014).

[14] W.L. Jang, Y.M. Lu, W.S. Hwang, W.C. Chen, *J. Eur. Ceram. Soc.* **30**, 503 (2010).

[15] R.D. Shannon, *Acta Cryst A.* **32**, 751 (1976).

[16] Yan Li, Xinhai Li, Zhixing Wang, Huajun Guo, Tao Li, *Ceram. Int.* **42**, 14565 (2016).

[17] R. Kayestha, K. Sumati, H.R. Kayestha, *FEBS Lett.* **368**, 285 (1995).

[18] V. Saravanan, P. Shankar, G.K. Mani, J.B.B. Rayapan, *J. Anal. Appl. Pyrolysis.* **11**, 272 (2015).

[19] F. Bayansal, H.A. Çetinkara, S. Kahraman, H.M. Çakmak, H.S. Güder, *Ceram. Int.* **38**, 1859 (2012).

[20] A.Y. Oral, E. Mensur, M.H. Aslan, *Mater. Chem. Phys.* **83**, 140 (2004).

[21] M. Stamataki, D. Mylonas, D. Tsamakis et al., *Sen. Lett.* **11**, 1964(2013).

[22] M. Kaur, K.P. Muthe, S.K. Despande et al., *J. Cryst. Growth* **289**, 670(2006).

[23] N. Mukherjee, B. Show, S.K. MAji et al., *Mater. Lett.* **65**, 3248 (2011).

[24] K.P. Muthe, J.C. Vyas, S.N. Narang et al., *Thin Solid Films* **324**, 37 (1998).

[25] M. Xu, L. Yang, Y. Li et al., *Physica B* **406**, 3180 (2011).

[26] F. Bayansal, T. Taskopru, B. Sahin, *Metallurg. Mater. Trans. A* **45**, 3670 (2014).

[27] N.M. Basith, J.J. Vijaya, L.J. Kennedy, M. Bououdina, *Mater. Sci. Semicond. Process* **17**, 110 (2014).

[28] F. Bayansal, Y. Gülen, B. Sahin, S. Kahraman, H.A. Çetinkara, *J. Alloys Compd.* **619**, 378 (2015).

[29] R.G. Kadhim, B.R.S. Kzar, *J. World Sci. News* **56**, 56 (2016).

[30] R.C. Wang, P.H. Huang, P.C. Chuang, Y.-C. Lin, *J. Electroanal. Chem.* **839**, 160 (2019).

[31] F. Bayansal, O. Sahin, H.A. Cetinkara, *Thin Solid Films* **697**, 137839 (2020).

[32] C.Y. Chiang, Y. Shin, S. Ehrman, *J. Electrochem. Soc.* **159**, B227 (2011).

[33] J. Iqbal, T. Jan, S. Ul-Hassan, I. Ahmed, Q. Mansoor, M.U. Ali, F. Abbas, M. Ismail, *AIP Adv.* **5**, 1632 (2015).

[34] S. Das, T.L. Alford, *J. Appl. Phys.* **113**, 244905 (2013).

[35] M.V. Zdorovets, D.B. Borgekov, I.E. Kenzhina, A.L. Kozlovskiy, *Phys. Lett. A* **382**, 175 (2018).

[36] D. Naveena, T. Logu, R. Dhanabal, K. Sethuraman, A. Chandra Bose, *J. Mater. Sci. Mater. Electron.* **30**, 561 (2019).

[37] R.D. Prabu, S. Valanarasu, H.A.H. Geno et al., *J. Mater. Sci. Mater. Electron.* **29**, 10921 (2018).

[38] B. Rahal, B. Boudine, Y. Larbah, N. Souami, *J. Inorg. Organomet. Polym. Mater.* **31**, 4001 (2021).

[39] A. Badawi, M.G. Althobaiti, S.S. Alharthi, A.M. Al-Baradi, *Phys. Lett. A* **411**, 127553 (2021).

[40] R.D. Shannon, *Acta. Cryst. A.* **32,** 751 (1976).

[41] H.A. Hussin, R.S. Al-Hasnawy, R.I. Jasim, N.F. Habubi, S.S. Chiad, *J. Green Eng.* **10**, 7018 (2020).

[42] Y. Larbah, M. Adnane, B. Rahal, *Semiconductors* **54**, 1439 (2020).

[43] I.A. Zghair, A.O. Al Khayatt, A. Asaad, Sh.K. Hussain, *Optik* (Stuttg) **19**, 48 (2019).

[44] Y.S. Yu, G.Y. Kim, B.H. Min, S.C. Kim, *J. Eur. Ceram. Soc.* **24**, 1865 (2004).

[45] J.I. Pankove, *Optical Processes in Semiconductors*, 2nd ed., Courier Dover Publication, New York 2010.

[46] V. Anand, A. Sakthivelu, K. Deva Arun Kumar et al., *Ceram. Int.* **44**, 6730 (2018).

[47] T.Z. Khodair, H.A. Adwan, H.N. Shallal, *Diyala J. Pure Sci.* **13**, 198 (2017).